Toward Computing Relative Configurations: 16-*epi*-Latrunculin B, a New Stereoisomer of the Actin Polymerization Inhibitor Latrunculin B

Thomas R. Hoye,*,[†] Seif-Eldin N. Ayyad,[‡] Brian M. Eklov,[†] Nadia E. Hashish,[§]
W. Thomas Shier,[§] Khalid A. El Sayed,[||] and Mark T. Hamann[||]

*Contribution from the Departments of Chemistry and Medicinal Chemistry,
University of Minnesota, Minneapolis, Minnesota 55455, Department of Pharmacognosy,
School of Pharmacy, The University of Mississippi, University, Mississippi 38677, and
Chemistry Department, Faculty of Science, Mansoura University, New Dammiatta, Egypt*

Received January 28, 2002

Abstract: The title compound, 16-*epi*-latrunculin B (**3**), has been isolated from the sponge *Negombata magnifica* collected from the Red Sea near Hurghada, Egypt. This new natural product was determined to be an epimer of latrunculin B (**1**), which was found in the same sponge collection. The structure of **3** was initially deduced from proton and carbon NMR chemical shift trends and proton−proton nuclear Overhauser effect experiments. The cytotoxicity (murine tumor and normal cell lines) and antiviral (HSV-1) properties of **3** and **1** were determined. A computational study applicable to this class of stereochemical problems was then investigated. Specifically, the complete set of vicinal and allylic coupling constants was calculated for each of the four diastereomers whose configurations differed at C(8) and C(16). These computed *J*'s were then compared with the experimental *J* values (28 in number) determined for **1** and **3**. This analysis resulted in the same assignment of relative configuration for compound **3** reached using the more classical methods. The validity of the method is established by the fact that the 28 computed coupling constants for (known) **1** and (newly determined) **3** varied from the experimental *J* values with an average of just 0.57 and 0.53 Hz, respectively. This strategy represents a general, powerful, and readily adoptable tool for determining the relative configuration of complex molecules.

Introduction

Latrunculin B (**1**), a potent inhibitor of actin polymerization,[1] was first isolated from the sponge *Latrunculia magnifica*, collected in the Gulf of Elat.[2] As reported in 1980, its structure was deduced by comparison of its NMR properties with those of the closely related vinylog, latrunculin A (**2**), for which a single-crystal X-ray structure determination was secured.[2,3] Working with a collection of *Negombata magnifica* from the Red Sea near Hurghada, Egypt, we recently isolated both **1** and a closely related new compound. The latter, which possesses antiviral activity toward herpes simplex type 1 virus (HSV-1) and cytotoxic properties against KA31T and NIH3T3 cell lines (see Supporting Information), was readily judged to be isomeric with **1** (high-resolution FABMS data implicated the molecular formula of the new compound as $C_{20}H_{29}NO_5S$). Its configuration

was assigned by interpretation of NMR chemical shift (proton and carbon) and nuclear Overhauser effect (NOE) data. We then undertook a computational study based on coupling constant analysis. The entire array of *experimental* vicinal and allylic proton−proton coupling constants[4] (*J*'s) was compared with appropriate sets of *computed J* values. The same structural assignment was reached using this nonclassical method of analysis. We suggest that this approach, which enhances traditional three-bond coupling constant ($^3J_{H,H}$) analysis through the integration of computational methods and quantitative comparisons,[5] represents a powerful strategy for the assignment of relative configuration to stereochemically complex molecules[6] even those containing macrocyclic rings and relatively large numbers of degrees of conformational freedom.[7] We have concluded that

* Corresponding author. E-mail: hoye@chem.umn.edu.
† Department of Chemistry, University of Minnesota.
‡ Mansoura University.
§ Department of Medicinal Chemistry, University of Minnesota.
|| The University of Mississippi.

(1) Latrunculins A and B now represent the most widely used tools for inhibition of actin polymerization in cell biology studies. Since the start of 2000, more than 100 primary publications concerning both latrunculin and actin have appeared.
(2) Kashman, Y.; Groweiss, A.; Shmueli, U. *Tetrahedron Lett.* **1980**, *21*, 3629−32.
(3) Jefford, C. W.; Bernardinelli, G.; Tanaka, J.; Higa, T. *Tetrahedron Lett.* **1996**, *37*, 159−62.

(4) (a) Hoye, T. R.; Hanson, P. R.; Vyvyan, J. R. *J. Org. Chem.* **1994**, *59*, 4096−103. (b) Hoye, T. R.; Zhao, H. *J. Org. Chem.* Published on web 05/14/2002.
(5) A powerful qualitative *J*-based approach, utilizing primarily three-bond carbon−proton coupling constant ($^3J_{C,H}$) analysis, has been developed[a] and applied[b−d] to the assignment of acyclic stereochemical relationships: (a) Matsumori, N.; Kaneno, D.; Murata, M.; Nakamura, H.; Tachibana, K. *J. Org. Chem.* **1999**, *64*, 866−76, and references therein. (b) Murata, M.; Matsuoka, S.; Matsumori, N.; Paul, G. K.; Tachibana, K. *J. Am. Chem. Soc.* **1999**, *121*, 870−1. (c) Wu, M.; Okino, T.; Nogle, L. M.; Marquez, B. L.; Williamson, R. T.; Sitachitta, N.; Berman, F. W.; Murray, T. F.; McGough, K.; Jacobs, R.; Colsen, K.; Asano, T.; Yokokawa, F.; Shioiri, T.; Gerwick, W. H. *J. Am. Chem. Soc.* **2000**, *122*, 12041−2. (d) Bassarello, C.; Bifulco, G.; Evidente, A.; Riccio, R.; Gomez-Paloma, L. *Tetrahedron Lett.* **2001**, *42*, 8611−3.

Table 1. Proton Chemical Shifts, Coupling Constants, COSY Correlations, and Chemical Shift Differences for Latrunculin B (**1**) and 16-*epi*-Latrunculin B (**3**) in CDCl₃[a]

	latruncul in B (**1**)				16-*epi*-latrunculin B (**3**)				
proton(no.)	δ (ppm)	mult	*J*'s (Hz)	COSY (to x[b])	δ (ppm)	mult	*J*'s (Hz)	COSY (to x[a])	$\Delta\delta = \delta_1 - \delta_2$ (ppm)
H(2)	5.69	q	1.5	19	5.67	q	1.5	19	+0.02
H(4a)	2.67	ddd	12.5, 12.5, 4.7	4′,5,5′	2.80	ddd	12.5, 12.0, 4.7	4′, 5, 5′	−0.13
H(4b)	1.98	ddd	12.5, 13.0, 4.7	4,5′,5	1.98	ddd	12.5, 12.7, 4.5	4, 5′, 5	0.00
H(5a)	2.33	dddd	14.0, 12.5, 11.5, 4.7	5′,4,6,4′	2.41	ddddd	14.5, 12.0, 11.7, 4.5, 1.0	5′,4,6,4′	−0.08
H(5b)	2.20	ddddd	14.0, 13.0, 4.7, 3.0, 2.2	5,4′,4,6, 7	2.17	ddddd	∼14, 12.7, 4.7, 2.7, 2.5	5,4′,4,6, 7	+0.03
H(6)	5.26	ddd	11.5, 11.5, 3.0	7,5,5′	5.25	ddd	11.7, 11.2, 2.7	7,5,5′	+0.01
H(7)	5.05	ddd	11.0, 11.0, 2.2	6,8,5′	5.04	dddd	11.2, 11.0, 2.7, 1.0	6,8,5′	+0.01
H(8)	2.64	m		7,9,9′,20	2.62	dddq	11.0, 10.7, 4.2, 6.5	7,9′,9,2 0	+0.02
H(9a)	1.72	dddd	13.7, 12.5, 3.7, 4.2	9′,8,10,1 0′	1.66	dddd	14.0, 12.7, 4.2, 4.0	9′,10′,8, 10	+0.06
H(9b)	1.11	dddd	13.7, 11.0, 4.2, 3.2	9,10,8,1 0′	1.14	dddd	14.0, 10.7, 4.0, 4.0	9,8,10′, 10	−0.03
H(10a)	1.49	dddd	14.0, 11.0, 3.7, 3.0	10′,9′,9, 11	1.50	dddd	14.0, 10.5, 4.0, 4.0	10′,11,9 ,9′	−0.01
H(10b)	1.37	dddd	14.0, 12.0, 4.2, 3.2	10,11,9, 9′	1.38	dddd	14.0, 12.7, 4.0, 2.7	10,9,9′, 11	−0.01
H(11)	4.24	dddd	∼12, ∼12, ∼3, ∼3	12′,10′,1 2,10	4.35	dddd	11.5, 11.5, 2.7, 2.2	12′,10,1 0′,12	−0.11
H(12eq)	1.75	dddd	14.0, 3.0, 2.2, 1.7	12′,11,1 3,14	1.72	dddd	13.7, 3.2, 2.2, 2.0	12′,13,1 1,14	+0.03
H(12ax)	1.53	ddd	14.0, 12.0, 2.5	12,11,13	1.54	ddd	13.7, 11.5, 2.5	12,11,1 3	−0.01
H(13)	5.46	dddd	3.5, 3.2, 3.0, 3.2	12,12′,1 4,14′	5.28	dddd	3.2, 3.2, 3, 2.5	14′,12,1 4,12′	+0.18
H(14eq)	2.09	ddd	14.7, 3.2, 2.0	14′, 13,12	2.20	ddd	14.5, 3.2, 2.0	14′,13,1 2	−0.11
H(14ax)	1.94	dd	14.7, 3.0	14,13	1.60	ddd	14.5, 3.5, 1.5	14,13,O H	+0.34
H(16)	3.84	ddd	9.0, 6.0, 1.0	17,17′,N H	3.87	ddd	8.5, 8.5, 1.0	17,17_, NH	−0.03
H(17a)	3.48	dd	11.7, 9.0	17′, 16	3.40	dd	11.5, 8.5	17_,16	+0.08
H(17b)	3.39	dd	11.7, 6.0	17, 16	3.28	dd	11.5, 8.5	17,16	+0.11
CH₃(19)	1.91	d	1.0	2	1.92	d	1.5	2	−0.01
CH₃(20)	0.96	d	6.5	8	0.97	d	6.5	8	−0.01
OH	3.85	brs		−	3.26	brs		14	+0.59
NH	5.66	brs		16	5.52	brs		16	+0.14

[a] Both spectra recorded at a concentration of ∼5 mM. [b] Correlation observed to proton H(x).

the new isomer is epimeric with latrunculin B (**1**) at C(16) (i.e., **3**). The arguments that support this conclusion are presented in the following discussion.

1
latrunculin B

2
latrunculin A

3
16-epi-latrunculin B
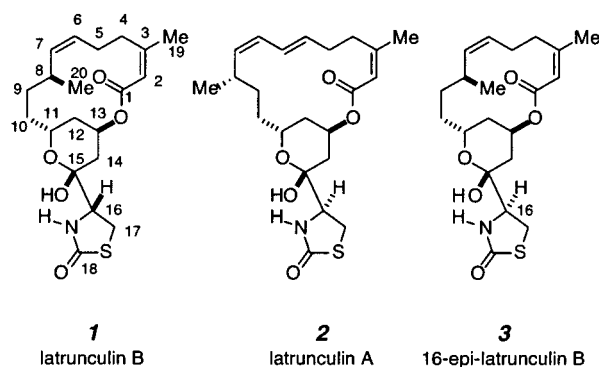
Chemical Shift and Nuclear Overhauser Enhancement Observations

Proton and carbon NMR data for both **1** and **3** are presented in Tables 1 and 2, respectively. At the outset we noticed discrepancies among previous reports of the proton chemical shift data described for latrunculin B (**1**).[1,8] We surmised and

Table 2. Carbon Chemical Shifts for Latrunculin B (**1**) and 16-*epi*-Latrunculin B (**3**) in CDCl₃

carbon no. (mult from DEPT)	δ (ppm)		
	latrunculin B (**1**)	16-*epi*-latrunculin B (**3**)	$\Delta\delta = \delta_1 - \delta_2$ (ppm)
1 (s)	165.54	165.77	−0.23
2 (d)	117.89	118.10	−0.21
3 (s)	154.72	155.42	+0.30
4 (t)	35.65	35.60	+0.05
5 (t)	26.72	26.66	+0.06
6 (d)	127.45	127.70	−0.25
7 (d)	135.70	135.51	+0.19
8 (d)	28.78	28.99	−0.21
9 (t)	30.99	31.13	−0.14
10 (t)	31.07	31.17	−0.10
11 (d)	62.37	62.92	−0.55
12 (t)	35.26	35.50	−0.24
13 (d)	68.54	67.68	+0.86
14 (t)	31.71	32.29	−0.58
15 (s)	97.40	96.49	+0.91
16 (d)	61.85	62.74	−0.89
17 (t)	28.56	28.93	−0.37
18 (s)	175.21	175.85	−0.64
19 (q)	24.06	24.44	−0.38
20 (q)	22.23	22.28	−0.05

then confirmed that there is a concentration dependence of the chemical shifts for a number of protons for **1** when measured in CDCl₃.[9] This phenomenon has been observed previously.[10]

(6) For another strategy that combines computational and spectroscopic methods, in this case based on molar rotations (or circular dichroism[d,e]), to provide a powerful technique for assignment of relative (and remote[d,e]) stereochemical relationships see a−d: (a) Kondru, R. K.; Lim, S.; Wipf, P.; Beratan, D. N. *Chirality* **1997**, *9*, 469−77. (b) Kondru, R. K.; Wipf, P.; Beratan, D. N. *Science* **1998**, *282*, 2247−50. (c) Kondru, R. K.; Wipf, P.; Beratan, D. N. *J. Am. Chem. Soc.* **1998**, *120*, 2204−5. (d) Specht, K. M.; Nam, J.; Ho, D. M.; Berova, N.; Kondru, R. K.; Beratan, D. N.; Wipf, P.; Pascal, R. A.; Kahne, D. *J. Am. Chem. Soc.* **2001**, *123*, 8961−6. (e) Nicholas, G. N.; Molinski, T. F. *J. Am. Chem. Soc.* **2000**, *122*, 4011−19.

(7) We previously used the computation[/3*J*H,H]-based strategy to assign the relative configuration of the otteliones (A and B), which, because of their bicyclo[4.3.0]nonane skeleton, were comparatively much more conformationally constrained: Ayyad, S.-E. N.; Judd, A. S.; Shier, W. T.; Hoye, T. R. *J. Org. Chem.* **1998**, *63*, 8102−6.

(8) (a) Groweiss, A. Shmueli, U.; Kashman, Y.; *J. Org. Chem.* **1983**, *48*, 3512−6. (b) Kashman, Y.; Groweiss, A.; Lidor, D.; Blasberger, D.; Carmely, S. *Tetrahedron* **1985**, *41*, 1905−14. (c) Blasberger, D.; Carmely, M.; Cojocaru, M.; Spector, I.; Shochet, N. R.; Kashman, Y. *Liebigs Ann. Chem.* **1989**, 1171−88. (d) Smith, A. B., III; Leahy, J. W.; Noda, I.; Remiszewski, S. W.; Liverton, N. J.; Zibuck, R. *J. Am. Chem. Soc.* **1992**, *114*, 2995−3007.

(9) This effect is seen principally in the chemical shifts of protons H(4), H(5), H(11), H(13), H(14), H(14′), H(17), and H(17′). ¹H NMR spectra of **1** in CDCl₃ were recorded at both ∼75 and ∼5 mM (see Table 1) concentrations, giving rise to the following $\Delta\delta$ (=$\delta_{75mM} - \delta_{5mM}$) values of greater than 0.03 ppm: H(4), 2.73(+0.06); H(5), 2.40(+0.07); H(11), 4.30(+0.06); H(12), 1.71(−0.04); H(13), 5.36(−0.10); H(14), 2.16(+0.07); H(14′), 1.84-(−0.10); H(17), 3.44(−0.04); and H(17′), 3.44(+0.05).
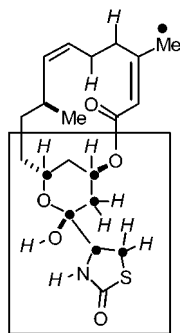
Figure 1. Protons (*H*) and carbons (●) having NMR chemical shift differences ($\Delta\delta$) of >|0.06| and |0.30| ppm, respectively, for latrunculin B (**1**) and the new isomer **3**.

Interestingly, proton NMR spectra of isomer **3** do not give evidence of any concentration-dependent chemical shifts over the same range of concentrations.[9]

Small but significant differences were observed in the chemical shifts of various protons and carbons in the NMR spectra of latrunculin B (**1**) and the new epimer **3**. These are shown as bold entries in the $\Delta\delta$ column of Tables 1 and 2 and as the indicated protons (for those having $\Delta\delta = \delta_1 - \delta_2 > \pm 0.06$ ppm) and dotted carbons (for those having $\Delta\delta = \delta_1 - \delta_2 > \pm 0.30$ ppm), respectively, in the structure shown in Figure 1. Taken together, these data suggested that the structural difference(s) between **1** and **3** reside(s) in the boxed region of that structure.

It was easily deduced that **1** and **3** had identical configurations among the stereocenters on the pyran ring as well as the same geometry of the two alkenes. This followed from (i) analysis of the vicinal coupling constants among the protons on C(11)−C(14) and C(6)−C(7) of the pyran ring and disubstituted alkene, respectively, and (ii) the NOE interaction between protons on C(2) and C(19) (the allylic methyl group). This, then, required that the new isomer be epimeric with **1** at either the C(8), methyl-bearing stereocenter; the C(16), thiazolidinone stereocenter; or both.

Given the density of larger chemical shift differences in the C(10)−C(18) region of the two molecules (see box in Figure 1), the most likely candidate was the C(16) epimer.

Thorough analysis of the NOESY data allowed identification of the nonvicinal enhancements indicated in Figure 2 within the partial structures **4** and **6** [i.e., C(11) through C(18)] for **1** and **3**, respectively. As with the chemical shift data, there is clearly a lack of parallelism in the NOE signatures of these two compounds, again suggesting that the two have different spatial relationships among the protons in the C(11)−C(18) region of the skeleton. All of the NOE's shown in **4** for latrunculin B can be accounted for by assuming magnetization transfer principally occurs through two conformations, **5a** and **5b**, which are rotamers about the C(15)−C(16) and C(15)−OH bonds. All of the NOE's shown in **6** for *epi*-latrunculin B can be accounted for through conformation **7**, in which each proton of the methylene pair at C(17) is simultaneously in proximity with each proton of the methylene pair at C(14). Thus, we have assigned the configuration at C(16) in the new isomer **3** as
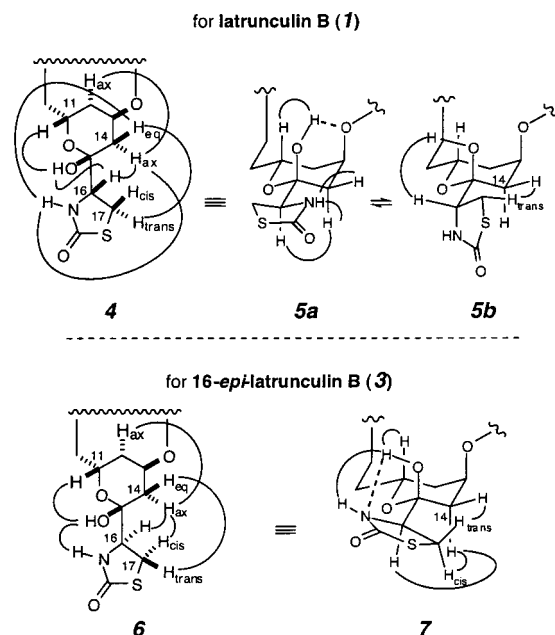
---

(10) Zibuck, R. Ph.D. Thesis, University of Pennsylvania, 1986. Also, communication with Professor Amos B. Smith, III. A copy of the ¹H NMR spectrum and an authentic sample of synthetic **1**, provided by Professor Smith, were quite helpful in resolving this initially perplexing discrepancy.

Figure 2. Observed NOE's within the C(11)−C(18) regions of latrunculin B (**1**) (top, **4** and **5**) and epimer **3** (bottom, **6** and **7**).

opposite (i.e., *S*) that at C(16) in latrunculin B (i.e., *R*), as shown in partial structures **6** and **7**.

Hydrogen Bonding Observations

Significant NMR spectroscopic properties were also observed for the hemiketal OH and thiazolidinone NH protons. For both isomers **1** and **3**, the OH was and the NH was not rapidly exchanged upon addition of D$_2$O to the CDCl$_3$ sample. However, in **3** this exchange was accompanied by a simplification of H(14ax) due to the loss of a 1.5 Hz coupling, which we then attributed to a long-range (W-type) coupling of H(14ax) with OH, consistent with the geometry of conformer **7** (Figure 2). In both **1** and **3**, the chemical shift of the OH proton itself in CDCl$_3$ (δ 3.85 and 3.26, respectively) is indicative that each is engaged as a hydrogen bond donor. We suggest that the hydroxyl proton in **3** (donor) interacts with π-electron density of the amide-like nitrogen (acceptor) as indicated with the dashed line in **7**. The location of this proton in the shielding region of the amide bond would also explain its higher field chemical shift vis-à-vis the OH in **1**. This also orients the OH close to the NH, as is required to account for the observed NOE between these two. By contrast, the OH in latrunculin B (**1**) is likely donating to the axial lactone ether oxygen at C(13) (dashed line in **5a**).[11] The presence of a strong NOESY cross-peak between the OH and C(11) axial proton in **1** is consistent with this arrangement, as is the fact that the H(13) methine proton in **1** is further downfield than it is in **3** (δ 5.46 vs 5.28, respectively). Upon addition of DMSO (∼200 equiv) to the CDCl$_3$ solution of **1**, the H(13) methine proton was shifted upfield to δ 5.21, consistent with disruption of the internal hydrogen bond to the lactone ether oxygen.

Relative Configuration of 3

On the basis of the evidence presented thusfar, we were confident that isomer **3** was epimeric with **1** at C(16). The

---

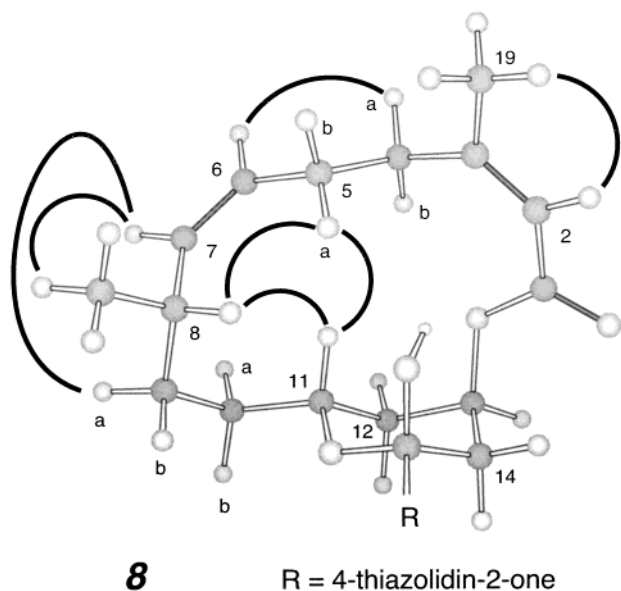(11) Kashman, Y.; Lidor, R.; Blasberger, D.; Carmely, S. *Tetrahedron Lett.* **1986**, *27*, 1367−70.

Figure 3. NOE interactions observed within the macrocyclic portion of *both* latrunculin B (**1**) and epimer **3**.

remaining stereochemical issue was whether the two had the same or opposite configuration at C(8). Given the great similarity in both the chemical shift and coupling constant data among protons residing from C(6)−C(10) in **1** and **3** (Table 1), we initially judged that the two had the same configuration at C(8). This hypothesis was further supported by comparison of nonvicinal NOE relationships within the macrocyclic lactone portion of the two molecules. Depicted in structure **8** in Figure 3 [which is the geometry of the global minimum energy conformation arising from molecular mechanics calculations of **1** (see later discussion)] is the set of NOE's that was observed in common for both of isomers **1** and **3**. As Kashman had deciphered through detailed and thorough analysis of coupling constant and NOE data,[8b] latrunculin B has a remarkably well-defined conformational preference for a structure very much like **8**.[12] That **1** and **3** share such a high degree of similarity in their NOE and coupling (see below) data, it is quite compelling that they share configuration at C(8). This is also consistent with the assignment of the structure of the new epimer as 16-*epi*-latrunculin B (**3**).

To probe whether latrunculin B (**1**) and 16-*epi*-latrunculin B (**3**) might readily interconvert, samples of pure **1** in CDCl$_3$ were incubated with either trifluoroacetic acid or triethylamine. Enolization of the ring-opened C(15)-ketone toward C(16) would, of course, be accompanied by epimerization of C(16). However, at room temperature no change was observed even after 1 month. When the samples were warmed to ∼50 °C for many days, partial decomposition to unidentified products ensued, but again there was no evidence of resonances arising from **3**. Had this experiment succeeded, it would have provided a handle for unambiguous determination of the absolute configuration of **3**. As it stands, we can only speculate that on biogenetic grounds it seems more reasonable that 16-*epi*-latrunculin B has the structure of **3** rather than the mirror image.

Computing the Relative Configuration of 16-*epi*-Latrunculin B (3): Correlation of Calculated and Experimental ^{1}H−^{1}H Coupling Constants

Assignment of relative *configuration* within relatively rigid molecular frameworks based upon analysis of three-bond

proton−proton coupling constant data is, of course, a time-honored method. Strategies for understanding *conformational* aspects of molecules with greater flexibility by combining *J* analysis with computational treatments are also plentiful.[13,14] However, the assignment of relative configuration within relatively flexible molecules based on coupling constant analysis has been largely limited to qualitative approaches. One very noteworthy example of this strategy is the "*J*-based configurational analysis" of Murata, which uses $^3J_{H,C}$ data to deduce relative configurational relationships, including those of remote stereocenters within acyclic subunits.[5]

We describe next a computational approach, in which sets of computed *J* values for each of several viable diastereoisomers are compared with the set of experimental coupling constants. This was studied in the context of the structure of the newly deduced, 16-*epi*-latrunculin B. To first test this approach, we compared computed with experimental *J*'s for latrunculin B itself to see if the method was valid for this class of compound.
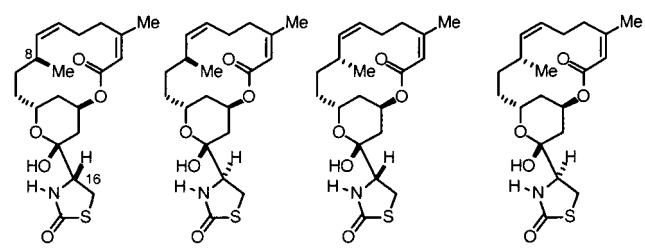
As summarized in Table 1, we were able to determine the value of every vicinal (and geminal) coupling constant for latrunculin B and for 16-*epi*-latrunculin B. In addition, longer range, four-bond couplings were identified between H(2)−H(19), H(5b)−H(7), and H(12eq)−H(14eq) in **1** and between H(2)−H(19), H(5b)−H(7), H(12eq)−H(14eq), and H(14ax)−OH in **3**. Our detailed analysis of the proton NMR coupling constants for latrunculin B suggested that the solution structure for its macrocyclic moiety in CDCl$_3$ is consistent with the conformation shown in structure **8** (Figure 3).[8b]

Latrunculin B was then subjected to an MM2*-driven Monte Carlo conformational search within MacroModel.[15] A family of ∼600 minima was identified; 41 of these structures fell within 3 kcal mol^{-1} of the global minimum energy conformer. The latter is structure **8** in Figure 3 (the thiazolidinone ring atoms have been deleted for clarity), numbered to make clear the correlation with the proton numbers listed in Table 1. We then used MacroModel "analyze nmr" functions to compute the Boltzman-weighted average coupling constants for all vicinal protons in **1**. There is a remarkably good fit between the experimental and calculated *J* values. Namely, 24 of the 28 computable *J*'s were within 1.0 Hz of the experimental value, three were within 1.0−2.0 Hz, and the last differed by 2.6 Hz. The average variance[16] was 0.57 Hz.

The "goodness of fit" can be quantified in a number of ways, but we have elected to represent it as a modified χ^2 value, $\chi^{2\prime}$,[7] which we define as the sum of the squares of the differences between the experimental and computed *J* values for each of

(12) (a) It is reassuring that the geometry we compute for the global minimum energy structure of the macrocyclic lactone portion of latrunculin B, namely, **8**, is consistent with the conclusions about conformation reached earlier by Kashman[8b] and is also similar to the geometry seen in the crystal structure data for latrunculin A (**2**).[8a,11b] (b) The conformation of latrunculin A (**2**) observed in its cocrystal with an actin monomer is also similar in geometry to **8**: Morton, W. A.; Ayscough, K. R.; McLaughlin, P. J. *Nat. Cell Biol.* **2000**, *2*, 376−8.

(13) See: Kamienska-Trela, K.; Wójcik, J. *Nucl. Magn. Reson.* **2000**, *30*, 132−80. Also, the analogous topical chapter in preceding volumes of this series of Specialist Periodical Reports of the Royal Society of Chemistry.

(14) A Boltzman-weighted, computed coupling constant approach has been used to study conformational aspects of acyclic polypropionate fragments, e.g.: Stenkamp, D.; Hoffmann, R. W.; Göttlich, R. *Eur. J. Org. Chem.* **1999**, 2929−36.

(15) Mohamadi, F.; Richards, N. G. J.; Guida, W. C.; Liskamp, R.; Lipton, M.; Caufield, C.; Chang, G.; Hendrickson, T.; Still, W. C. *J. Comput. Chem.* **1990**, *11*, 440−67.

(16) The average of the *absolute values* of the differences in all 28 coupling constants [$(\Delta J)_{av} = (\Sigma|J_{exp} - J_{calc}|)/28$].

Table 3. $\chi^{2\prime}$ [$=\Sigma(J_{exp} - J_{calc})^2$] Values Derived from Experimental (CDCl$_3$) *J* Values for Latrunculin B (Entries 1−4) and 16-*epi*-Latrunculin B (Entries 5−8) vs Computed *J* Values for Latrunculin B (**1**), 16-*epi*-Latrunculin B (**3**), 8-*epi*-Latrunculin B (**9**), and 8,16-*bisepi*-Latrunculin B (**10**)

| | **1** | **3** | **9** | **10** |
| | latrunculin B | 16-*epi*-latrunculin B | 8-*epi*-latrunculin B | 8,16-*bisepi*-latrunculin B |

| | | $\chi^{2\prime}$ | |
entry	data sets	no solvation	CHCl$_3$ solvation
1	**1**$_{exp}$ vs **1**$_{calc}$	**19**	**23**
2	**1**$_{exp}$ vs **3**$_{calc}$	27	35
3	**1**$_{exp}$ vs **9**$_{calc}$	158	207
4	**1**$_{exp}$ vs **10**$_{calc}$	148	182
5	**3**$_{exp}$ vs **3**$_{calc}$	**21**	**25**
6	**3**$_{exp}$ vs **1**$_{calc}$	29	26
7	**3**$_{exp}$ vs **9**$_{calc}$	166	212
8	**3**$_{exp}$ vs **10**$_{calc}$	153	189

the protons.[17] The $\chi^{2\prime}$ value from comparison of the 28 computed vs experimental *J* values for latrunculin B is 19 or 23 for the two theoretical data sets calculated using either no solvation or CHCl$_3$ solvation, respectively, during the MM2* Monte Carlo runs. These are strikingly small values (i.e., good fits). This situation gave us confidence to apply the approach to the new structure **3**.

Prior to completing the NOE studies described above, we had established that the only stereocenters at which the new *epi*-latrunculin B isomer could differ from latrunculin B was at either C(8) or C(16) (or both). This was because it was clear that the relative configurations of the C(11), C(13), and C(15) centers within the rigid tetrahydropyran ring were identical in **1** and **3** as were the *E/Z* geometries of the $\Delta^{2,3}$ and $\Delta^{6,7}$ alkenes. We therefore performed analogous Monte Carlo conformational analyses and coupling constant calculations for each of 8-*epi*-, 16-*epi*-, and 8,16-*bisepi*-latrunculin B (**9**, **3**, and **10**, respectively). The experimental *J* values for the new latrunculin B isomer (as well as for latrunculin B itself) were compared with each of the calculated sets of *J*'s for **1**, **3**, **9**, and **10**. The resulting complement of $\chi^{2\prime}$ values is presented in Table 3.

The goodness of fit data are compelling for ruling out C(8) epimers. As was the case for the comparison of experimental with calculated *J* values for **1** (see above and entry 1, Table 3), the $\chi^{2\prime}$ for **3** (entry 5) is also decidedly smaller than for those possibilities epimeric at C(8) (entries 7 and 8). That is, the computed set of *J* values for 16-*epi*-latrunculin B matches the set of experimentally observed *J*'s for the new isomer far better (the average and maximum difference in *J* values is 0.53 and 3.3 Hz, respectively) than it does those for 8-*epi*-latrunculin B (**9**) or 8,16-*bisepi*-latrunculin B (**10**).

Conclusion

In the work described here we have benchmarked methodology that involves comparison of computed with experimental

NMR coupling constant data by applying it to known structures (i.e., **1** and **3**). This success raises the prospect of using this approach to assign the relative configuration of *new* compounds (either natural or synthetic in origin) bearing multiple stereocenters. Empirical approaches involving the use of chemical shift correlations to assign the configuration of stereochemically complex molecules are also valuable.[18] More recently, powerful universal NMR database methodology has been developed.[19] When applied to sophisticated molecules, some of these approaches require the sometimes onerous task of stereoselective synthesis of all members of a diastereomeric set of model compounds. Nonetheless, that investment is often well-warranted given the value of the resulting data set. Complementary computational/NMR methods such as the one described here have the prospect of allowing reliable stereochemical assignments to be made without the preparative burden. We are further assessing and developing the applicability of this strategy to other known and unknown structural types.

Experimental Section

Computational Methods. All calculations were performed with MacroModel 6.0 from Schrödinger, Inc. on an SGI O$_2$ (R5000) workstation.[20] A starting structure for each diastereomer was first minimized to a local minimum using the MM2* force field. The Monte Carlo search was configured using the "normal" sequence within the "automatic setup" routine in MacroModel. The following degrees of freedom were added. The (default) constrained torsion about the ester was removed [i.e., C(13)−O−C(1)=O], two closure bonds [C(15)−O, C(19)−S] were added to the one automatically identified by MacroModel [C(5)−C(6)], and six torsion bonds were added [C(1)−O, C(11)−C(12), C(12)−C(13), C(13)−C(14), C(16)−N, C(16)−C(17)] to the nine [C(1)−C(2), C(3)−C(4), C(7)−C(8), C(8)−C(9), C(9)−C(10), C(10)−C(11), C(13)−O, C(15)−O(H), C(15)−C(16)] automatically identified by MacroModel. These additions removed the "problematic flexible ring" condition present when only the default closure and torsion bonds were used. Each diastereomer was then subjected to a 10 000 iteration Monte Carlo search (500 steps /iteration) also using the MM2* force field and the PR conjugate gradient (PRCG) with no solvation and again with chloroform solvation. All minimized structures with energies greater than 50 kJ mol^{-1} of the global minimum were discarded. Typically, ~600−1000 unique conformations were found for each of the diastereomers, and ~50% had converged (to 0.05

(17) This $\chi^{2\prime}$ prime [$\chi^{2\prime} = \Sigma(A_{obsd} - A_{expected})^2$] differs slightly from the usual χ^2 value used in least-squares analysis, which is the sum of the squares of the differences between observed and expected values *divided by the expected value* (i.e., $\chi^2 = \Sigma[(A_{obsd} - A_{expected})^2/A_{expected}]$). In the present context, use of the usual χ^2 would have the effect of enhancing the importance of small *J* values, which we feel is not warranted.

(18) For examples see the following: (a) Palytoxin: Cha, J, K,; Christ, W. J.; Finan, J. M.; Fujioka, H.; Kishi, Y.; Klein, L. L.; Ko, S. S.; Leder, J.; McWhorter, W. W., Jr.; Pfaff, K.-P.; Yonaga, M.; Uemura, D.; Hirata, Y. *J. Am. Chem. Soc.* **1982**, *104*, 7369−71, and immediately preceding papers. (b) Syn/anti 1,3-diols: Hoffmann, R. W.; Weidmann, U. *Chem. Ber.* **1985**, *118*, 3980−92. (c) Acetogenins: Hoye, T. R.; Suhadolnik, J. C. *J. Am. Chem. Soc.* **1987**, *109*, 4402−3. (d) ^{13}C acetonide analysis: Rychnovsky, S. D.; Skalitzky, D. J. *Tetrahedron Lett.* **1990**, *31*, 945−8. Evans, D. A.; Rieger, D. L.; Gage, J. R. *Tetrahedron Lett.* **1990**, *31*, 7099−100. (e) AAL toxins: Boyle, C. D.; Harmange, J.-C.; Kishi, Y. *J. Am. Chem. Soc.* **1994**, *116*, 4995−6. (f) Fumonisin backbone: Hoye, T. R.; Jiménez, J. I.; Shier, W. T. *J. Am. Chem. Soc.* **1994**, *116*, 9409−10.

(19) Kobayashi, Y.; Lee, J.; Tezuka, K.; Kishi, Y. *Org. Lett.* **1999**, *1*, 2177−80. Also subsequent papers in this series through the most recent: Kobayashi, Y.; Hayashi, N.; Kishi, Y. *Org. Lett.* **2002**, *4*, 411−4.

(20) (a) The overall strategy is not confined to any particular software. Thus, many other packages capable of multi-conformational searches could be used, the environmentally adapted coupling constants could be assigned for each conformation geometry using modified Karplus relationships,$^{b-d}$ and the energetically weighted average *J* values can be determined "by hand" with the aid of standard spreadsheet software. (b) Karplus, M. *J. Chem. Phys.* **1959** *30*, 11−5. (c) Haasnoot, C. A. G.; DeLeeuw, F. A. A. M.; Altona, C. *Tetrahedron* **1981**, *36*, 2783−92. (d) Garbisch, E. W., Jr. *J. Am. Chem. Soc.* **1964**, *86*, 5561−4.

kJ Å^{-1} mol^{-1}). Each of these sets of minima was then subjected to several rounds of reminimization (typically 3−5 rounds, PRCG, MM2*, 1000 steps in each round) until over 90% of the minima had reached "good convergence" (to 0.0001 kJ Å^{-1} mol^{-1}). Each final family of conformers was used to obtain Boltzmann-weighted average ^{1}H-^{1}H coupling constants for all vicinal and allylic relationships using the "CoplF" routine (at 300 K) in the NMR subroutine of the Analyze mode. The coupling constant data were entered into an Excel spreadsheet and utilized to calculate the $\chi^{2\prime}$ values.

Supporting Information Available: All experimental details relating to isolation, purification, spectroscopic, and biological aspects of the work and tables (4) of the raw ΔJ ($= J_{\text{exp}} - J_{\text{calc}}$) values and the calculations used to reach the $\chi^{2\prime}$ values summarized in Table 3 (PDF). This material is available free of charge via the Internet at http://pubs.acs.org.

JA025734L